Journal of Hazardous Materials 384 (2020) 121361

Contents lists available at ScienceDirect

Journal of Hazardous Materials

journal homepage: www.elsevier.com/locate/jhazmat

Silica nanoparticles exacerbates reproductive toxicity development in high-fat diet-treated Wistar rats

Lianshuang Zhang[a,c,1], Jialiu Wei[a,d,1], Junchao Duan[a,b,1], Caixia Guo[b], Jin Zhang[a,b], Lihua Ren[a,b], Jianhui Liu[a,b], Yanbo Li[a,b,*], Zhiwei Sun[a,b], Xianqing Zhou[a,b,*]

[a] Department of Toxicology and Sanitary Chemistry, School of Public Health, Capital Medical University, Beijing, China
[b] Beijing Key Laboratory of Environmental Toxicology, Capital Medical University, Beijing, China
[c] Department of Histology and Embryology, Binzhou Medical University, Yantai, China
[d] Key Laboratory of Cardiovascular Epidemiology & Department of Epidemiology, Fuwai Hospital, National Center for Cardiovascular Diseases, Chinese Academy of Medical Sciences and Peking Union Medical College, Beijing, China

GRAPHICAL ABSTRACT

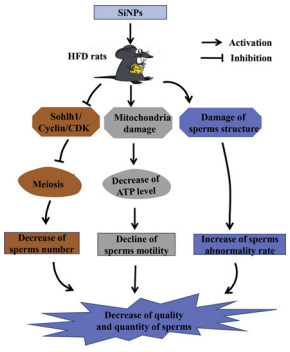

ARTICLE INFO

Editor: R. Debora.

Keywords:
Silica nanoparticles
Wistar rats
Meiosis process
Risk assessment
Energy metabolism dysfunction

ABSTRACT

To demonstrate the combined adverse effect and the mechanism of silica nanoparticles (SiNPs) with 57.66 ± 7.30 nm average diameter and high-fat diet (HFD) on Wistar rats, 60 male Wistar rats were randomly divided into six groups (n = 10): Control group, SiNPs group, HFD group, 2 mg kg^{-1} SiNPs + HFD group, 5 mg kg^{-1} SiNPs + HFD group and 10 mg kg^{-1} SiNPs + HFD group. HFD was administrated for 2 weeks for the rats in advance and SiNPs were supplied every 3 d for 48 d subsequently. The present study illustrated that both HFD and SiNPs could decrease sperm concentration, mobility rates, increase abnormality rates, damage testicular structure, reduce spermatogonium numbers and spermatoblast numbers, reduce ATP levels, and affect expression of regulatory factors for meiosis in testis. HFD and SiNPs further damaged the sperm and lowered the ATP level and expression of factors associated with meiotic signaling pathway compared with the HFD without SiNPs in testicular tissue of Wistar rats. These results suggested that SiNPs significantly promoted reproductive toxicity induced by HFD in Wistar rats, which provides novel experimental evidence and an explanation for magnified reproductive toxicity triggered by SiNPs in HFD rats.

* Corresponding authors at: Department of Toxicology and Sanitary Chemistry, School of Public Health, Capital Medical University, Beijing, 100069, China.
E-mail addresses: ybli@ccmu.edu.cn (Y. Li), xqzhou@ccmu.edu.cn (X. Zhou).
[1] These authors contributed equally to this work.

https://doi.org/10.1016/j.jhazmat.2019.121361
Received 14 July 2019; Received in revised form 26 September 2019; Accepted 28 September 2019
Available online 01 October 2019

1. Introduction

Natural silica nanoparticles (SiNPs) have been proved to be considered as the main inorganic ingredient of particulate matter pollution sources from air (Duan et al., 2016). Air pollution has been a serious social problem that poses the threat to human health and wildlife. SiNPs in the air are mainly from road dust, construction dust and industry (Duan et al., 2016; Feng et al., 2019; Shen et al., 2016). A recent study showed that exposure to pollutants from air can reduce reproductive performance (Liu et al., 2018). In more recent decades, the prevalence of infertility has increased dramatically (Sengupta et al., 2017). However, statistics illustrated that male factors, accounting for about 40% of all cases, contribute to infertility greatly (Lafuente et al., 2016). The continuous serious problem about human reproductive dysfunction including the decrease of human semen quality and sperm count has aroused strong reaction worldwide (Agarwal et al., 2015; Miura et al., 2017). Hence, it is urgent to understand the reason for disorder of the male productive system.

Evidence suggested that nanoparticles (NPs) could exert detrimental effect on human reproductive production. Animal studies have demonstrated that exposure to SiNPs by oral gavage induced decrease of number of Leydig cells and sperm motility and normal sperm morphology in rats (Baki et al., 2014). Our previous study found that SiNPs influenced maturation process of sperm in the epididymis, decreased the quantity and quality of epididymis sperm and led to energy metabolism dysfunction resulting from damage of mitochondria structure in mice by injection via the tail vein (Xu et al., 2014). However, the specific pathological mechanism of SiNPs-induced dysfunction of reproductive system is still unclear.

Currently, the increasing prevalence of obesity has been considered an epidemic worldwide (Deshpande et al., 2018). Obesity is linked closely with various health issues including diabetes, hypertension, cancer, and even disruption of the reproductive system (Luo et al., 2019; Li et al., 2018; Zhang and Zhou, 2019). World Health Organization (WHO) evaluated the overall global prevalence of primary infertility ranging from 8 to 15% (Aiceles and da Fonte Ramos, 2016). Studies showed that male obesity impacts on sperm motility and a negative correlation between obesity and male fertility status has been demonstrated (Paoli et al., 2019). Furthermore, growing evidence suggested that Body Mass Index (BMI) and odds of overweight or obesity increased significantly in childhood or adolescence when they were exposed particulate matter from air pollution during childhood (Mao et al., 2016). A study found that men whose BMI were greater than 25 kg/m^2 had a significant amount of lower total sperm than those with normal weight (Aggerholm et al., 2008). However, researches on the reproductive toxicity induced by SiNPs on obesity populations have not yet been launched.

During spermatocytogenesis, the spermatogonia divides through mitosis to form two diploid cells called primary spermatocytes. The primary spermatocytes undergo meiosis I and split to form two diploid daughter cells as the parent cell. The resulting secondary spermatocytes then go through meiosis II to form round spermatids. The process by which spermatogonium becomes sperm is called spermatogenesis (Valbuena et al., 2008; Walker and Cheng, 2005). Sohlh1 is a differentiation factor controlling the switch on meiosis in mammals, which is required for spermatogonial differentiation (Matson et al., 2010; Ballow et al., 2006). Cyclin-dependent kinases (CDKs) have critical roles in meiotic cell cycle progression in eukaryotes (Campsteijn et al., 2012). It has been reported that Sohlh1 can inhibit the meiosis process through regulating the expression of CDKs, thereby decreasing the amount of sperm and inducing reproductive toxicity (Guo et al., 2016). However, whether Sohlh1 and CDKs are involved in the SiNPs-caused reproductive toxicity in obese individuals is still unknown.

Overall, the present study aimed to investigate the effect of SiNPs on reproductive toxicity and its mechanism in high-fat diet (HFD) Wistar rats. Our study will provide persuasive evidence for the potential mechanism of male reproductive toxicity in HFD Wistar rats induced by SiNPs.

2. Materials and methods

2.1. Experimental design

Experimental animals was obtained from Experimental Animal Center of Military Medical Sciences. 60 healthy male Wistar rats weighing 180–220 g were divided into 6 groups randomly. The rats were aged 6–7 weeks with mean weight of 200 ± 20 g. Every three rats were raised in a polysulfone (PSU) box (47 cm × 30 cm × 15 cm) in a ventilated environment (22℃ ± 2℃, 60% ± 10% relative humidity, 12 h light/dark cycle). The pads of the rats were replaced twice per week. After one-week adaption, the animals were randomly divided into six groups equally. Group II, IV, V and VI were received HFD for 2 weeks in advance to achieve hyperlipidemia models. After that, the four groups (II, IV, V and VI) were treated with 0, 2, 5 and 10 mg/kg·bw SiNPs suspensions, respectively. Group III was given 10 mg/kg·bw SiNPs suspension and group I (control group) was provided normal saline. As air pollutants getting into our bodies through respiratory tract and lungs, all of them were treated every 3 days for 48 d in total (16 times) by intratracheal instillation to more closely mimic human exposures. The dosage of SiNPs in vivo (2, 5, or 10 mg/kg·bw) in the current study was in reference to a sub-chronic rat inhalation study, in which the low dosage of SiNPs (2 mg/kg·bw) was converted according to WHO clean air standards, the respiratory rate and respiratory capacity of rat, as well as the safety coefficient from experimental animals extrapolated to humans (Du et al. (2013)). The dosage level difference is 2–10 times according to design principle of toxicology experiment. The HFD contained 1% cholesterol, 10% proteins, 10% lard oil, 0.2% cholate, 0.2% propylthiouracil, 5% carbohydrates and 73.6% basal diet (Kim et al., 2008). The rats were euthanized after 48 days and testicles and epididymides were collected. All the animal experiments were performed in accordance with the Health Guide of Capital Medical University for the Care and Use of Laboratory Animals, and the protocol was approved by the Committee on the Ethics of Animal Experiments of the Capital Medical University, Beijing, China (Ethical review number: AEEI-2014-068).

2.2. SiNPs preparation and characterization

SiNPs existing in an aqueous suspension were prepared by employing the Stöber method by College of Chemistry, Jilin University, China. The preparation of SiNPs was described in accordance with our previous laboratory study (Guo et al., 2015). Briefly, 2.5 mL tetraethylorthosilicate (TEOS) (Sigma, USA), 50 mL ethanol solution, 2 mL ammonia and 1 mL water were mixed, followed by the 2.5 mL tetraethyl orthosilicate adding to the mixture. The mixture mentioned above was sustained at 40 ˚C for 12 h with constant stirring (150 rpm), then the particles were centrifugated for 15 min (12,000 r/min), washed with deionized water three times and finally dispersed in 50 mL deionized water. Furthermore, to avoid aggregation of SiNPs, biodegradable and lower critical micelle concentration surfactants were employed in accordance with the procedure described in a previous study (Melvin et al., 2010). Finally, the surfactants were washed off, and the SiNPs suspensions were sonicated by a sonicator (160 W, 20 kHz, 5 min) (Bioruptor UDC-200; Diagenode, Liège, Belgium) prior to the addition to dispersion solution and performing tracheal perfusion so as to relieve the possible aggregation. The method of dispersion was in reference to the research of Guo et al (Guo et al., 2015). Moreover, the results from the agglomeration study were as the same as in the dispersion in medium. The size and distribution of SiNPs were measured by transmission electron microscopy (JEOL JEM2100, Japan) and Image J software (National Institutes of Health, USA). The zeta potential and hydrodynamic sizes of SiNPs were measured using a Zetasizer to

measure the stability of nanoparticles (Nano ZS90; Malvern Instruments, Malvern, UK). Moreover, gel-clot limulus amebocyte lysate assay kit for endotoxin test in SiNPs suspensions was obtained from Zhanjiang Bokang Marine Biological Co. Ltd (Zhanjiang, China).

2.3. Evaluation of sperms in epididymides

Sperms were extracted from epididymides and immediately incubated in Dulbecco's Modified Eagle Medium (2 mL) at 37°C for 5 min, followed by the concentrations and motility being measured by semen analyzer (Hamilton Thorne IVOS-II; Hamilton Thorne Research, Beverly, MA, USA). A smear of the sperm suspension was made on the glass. As for sperm deformation of sperms, we calculated the number among 1000 sperms under a high magnification microscope by counting. The sperm malformation rate = the amount of malformed sperm/1000 × 100%. Sperm were scored as normal or abnormal using the Kruger strict criteria.

2.4. Histological structure and ultrastructure of testes

The fixed testes in Bouin's fixation fluid was dehydrated with various concentrations (50, 70, 80, 90 and 100%) of alcohol in turn. The samples were then cleared with dimethyl benzene, embedded in paraffin, sectioned at a thickness of 5 μm (Leica RM2245, Germany), and stained with hematoxylin and eosin (H&E) for histological assessment. After staining, the slides were observed under the optical microscope (Olympus X71-F22PH, Japan). Ten visual fields from each sample of six were used to calculate the numbers of spermatogenic cells (spermatogonia, primary spermatocytes, secondary spermatocytes and spermatids) and measure the diameters of seminiferous tubules using cross-bonded method (Martins and Silva, 2001). The identification of different types of spermatogenic cells were based on our previous method (Jin Zhang et al., 2016).

As for ultrastructure, the testicle was fixed by 2.5% glutaraldehyde for 30 min. After being cut into small pieces, it was moved to the 2.5% glutaraldehyde at 4 °C overnight. The pieces washed by phosphate buffer (pH = 7.2) thrice were dehydrated by ethanol subsequently. Then the samples were embedded with Epon 812 and sliced by an LKB-V microtome followed by stained with 3% uranyl acetate-lead citrate. Finally, the ultrastructure of testes was observed using a transmission electron microscope (JEM2100, JEOL, Japan).

2.5. Measurement of ATP levels

The testicular tissue was washed by iced PBS (pH = 7.0) for removing blood and then grinded in 5 ml pre-cooled PBS. The homogenate was centrifuged at 12,000 rpm 4 °C for 10 min and ATP level was measured by a firefly luciferase-based ATP assay kit (Jiancheng, China) in accordance with the manufacturer's protocols. Finally, the luminance (RLU) was immediately detected by a Turner BioSystems luminometer (Promega Corporation, Madison, WI, USA).

2.6. Determination of protein expression involved in meiosis process

To determine the expression of Sohlh1 (38 kDa)/Cyclin A1 (52 kDa)/Cyclin B1 (48 kDa)/CDK 1 (34 kDa)/CDK 2 (34 kDa), western blots were performed. Briefly, the proteins extracted from testicular tissue were used a Protein Extraction kit (KeyGen, China) and determined by the bicinchoninic acid (BCA) protein assay (Dingguo Changsheng Biotech Co. Ltd, China). Equal amounts of lysate proteins (20 μg) were electrophoresed by 12% SDS − PAGE and transferred to polyvinylidene fluoride (PVDF) membranes (Millipore, USA) subsequently. After the membranes being blocked with 5% BSA for 2 h at room temperature and then incubated with rabbit-anti-Sohlh1 (1:500; Abcam, USA), rabbit-anti-Cyclin A1 (1:500, Bioss, China), rabbit-anti-CyclinB1 (1:500, Bioss, China), rabbit-anti-CDK1 (1:500, bioss, China), rabbit-anti-CDK2 (1:500,bioss,China), rabbit-anti-β-Actin (1: 1000; Santa Cruz, USA) overnight at 4 °C. The membrane was washed three times with TBST for 10 min each time and incubated with a secondary antibody (1: 5000; Proteintech, USA) at room temperature for 1 h. At last, ECL Chemiluminescence reagent (Pierce, USA) was used to find the protein bands (normalized with those of β-actin). Image J Software was used for densitometric analysis of protein bands.

2.7. Statistical analysis

All data were analyzed using the SPSS 17.0 software. An independent-samples *T*-test was used to analyze the differences between control and HFD and between control and SiNPs groups. One-way analysis of variance (ANOVA) was used to compare the significant difference among HFD groups treated with various doses of SiNPs, followed by least significant difference (LSD) test to compare the differences between various groups. The results were produced from ten independent Wistar rats per group made in triplicate per index. All significant differences were considered at $p < 0.05$. Data were expressed as means ± standard deviations.

3. Results

3.1. Characterization of SiNPs

The average diameter of SiNPs is 57.66 ± 7.30 nm (Fig. 1). SiNPs were endotoxin-free. The shape of SiNPs was near-spherical and dispersed equably in distilled water. The hydrodynamic sizes and zeta potentials of SiNPs detected in the distilled water, physiological saline and Dulbecco's Modified Eagle Medium appeared to be good monodispersity and excellent stability, and these findings were as the same as the descriptions reported by Guo et al (Guo et al., 2015).

3.2. The ATP levels alteration

As shown in Fig. 2, HFD could significantly decrease the ATP level in testicular tissue ($p = 0.01$) and SiNPs isolated had the same effect on it apparently ($p = 0.025$). SiNPs at all dosages (2, 5 and 10 mg/kg·bw) significantly decreased ATP levels in HFD rats, which firmly indicated that SiNPs further reduced ATP levels in HFD rats ($p < 0.01$).

3.3. Changes of epididymal sperm parameters

The sperm concentration significantly decreased from $10{,}575 \times 10^4\,mL^{-1}$ in control group to $7466.67 \times 10^4\,mL^{-1}$ in HFD group ($p = 0.012$), while SiNPs contributed to the downtrend and led it to reach bottom by $2916.67 \times 10^4\,mL^{-1}$ at 5 mg/kg·bw dosage in HFD rats ($p < 0.01$). As for the sperm motility rate, HFD apparently reduced it by 33% which is less than half of it compared with the control group, and it reached to bottom in the HFD + 5 mg/kg·bw SiNPs group as well ($p < 0.01$). Furthermore, HFD significantly promoted the sperm abnormality rate ($p = 0.005$), while SiNPs (5 and 10 mg/kg·bw) could magnify the sperm abnormality rate of the HFD rats (Table 1) ($p < 0.01$).

3.4. Changes in histological structure

In the control group, the basement membrane of the seminiferous tubules was smooth and integrity, and sperms were distributed evenly in the lumen of seminiferous tubule (Fig. 3A). In the HFD group, the shape and arrangement of spermatogenic cells were irregular and the decrease of mature sperm in the lumen was obviously observed (Fig. 3B). As for the SiNPs group, the seminiferous epithelium was thinner and few mature sperms could be found in the lumen (Fig. 3C). In the SiNPs groups with HFD diet (HFD + 2, 5 mg/kg·bw SiNPs), the more irregular and obscure shape as well as arrangement of

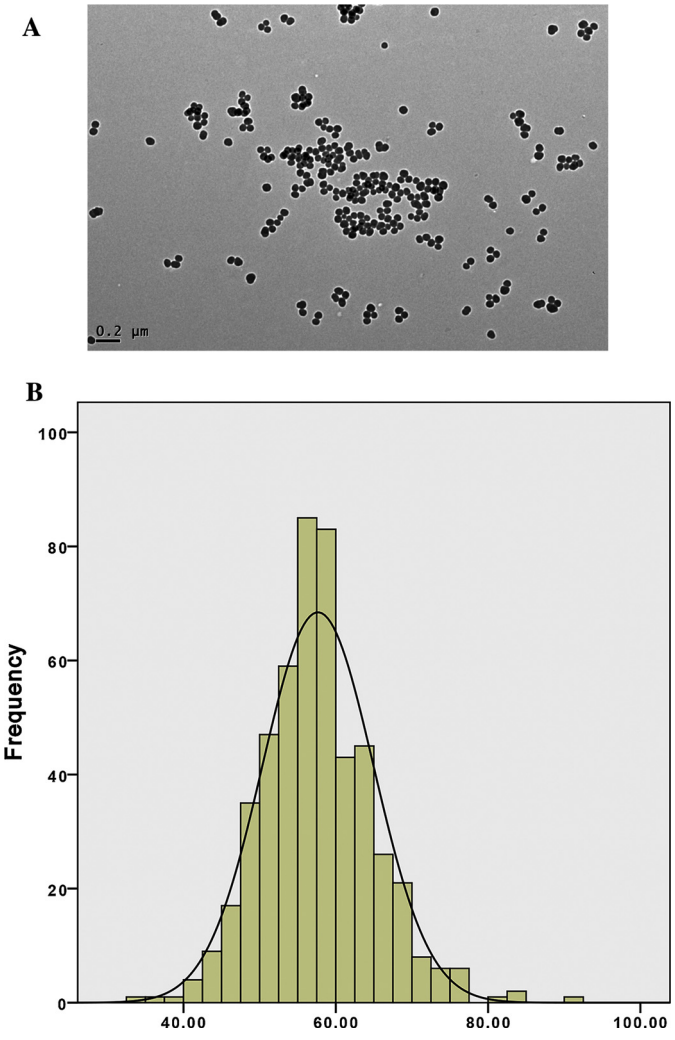

Fig. 1. Characterization of silica nanoparticles. (A) Transmission electron microscope shows silica nanoparticles appeared near-spherical shape and well monodispersity. (B) Normal distribution diagram with a mean diameter of 57.66 ± 7.30 nm. Data are expressed as means ± S.D from 500 independent nano silica particles. The data showed in the figure are representative.

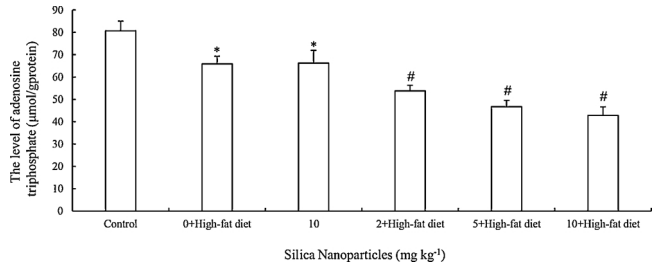

Fig. 2. Effects of different doses of silica nanoparticles on ATP level of testicular tissue in high-fat diet Wistar rats. * indicates remarkable difference compared with the control group, # indicates significant difference compared with the high-fat diet group. N = 10 per group, Data are expressed as means ± S.D. from three independent experiments per index. The data showed in the figure are representative. ($p < 0.05$).

spermatogenic cells were observed compared with the HFD group without SiNPs treatment (Fig. 3D, E). Furthermore, in the HFD + 10 mg/kg·bw SiNPs group, the seminiferous epithelium was thinner, some spermatogenic cells desquamated to the center of the lumen, and the gap of the spermatogenic cells increased significantly in the seminiferous tubule (Fig. 3F).

3.5. Changes of seminiferous tubule parameter

HFD intake could significantly decrease the seminiferous tubule diameter ($p = 0.030$) and spermatoblasts number ($p = 0.014$) and elevate the spermatogonium number ($p = 0.012$), and there was no obvious effect on the primary spermatocyte number when compared with the control group ($p = 0.896$). SiNPs meaningfully reduced the spermatogonium number ($p = 0.036$) and spermatoblasts number ($p = 0.001$) while had no effect on the seminiferous tubule diameter ($p = 0.926$) and primary spermatocyte number ($p = 0.797$). Furthermore, SiNPs could promote to decrease spermatogonium number, primary spermatocyte number and spermatoblasts number. Among the HFD rats, the spermatogonium number was most significantly increased by 5 mg/kg·bw SiNPs groups ($p = 0.011$). The primary spermatocyte number reached to bottom in 2 mg/kg·bw SiNPs group ($p = 0.043$). The spermatoblasts number with 2 mg/kg·bw SiNPs treatment was decreased most significantly ($p = 0.001$).

3.6. Changes in ultrastructure of testes

Mitochondria integrity and smoothness and the mitochondrial cristae clearly arranged in regular folds were observed in the control group. The microtubules of the cross section of sperm tails maintained the "9 + 2" structure explicitly (Fig. 4A, B). In the HFD group, the mitochondrial cristae partially disappeared, and the outer membrane of the mitochondria was ruptured. Moreover, the shape of microtubules of the sperm tails was damaged partly and the "9 + 2" structure was obscure even lost (Fig. 4C, D). As for the SiNPs group, the mitochondria swelled, mitochondrial cristae vanished, and vacuolization appeared. The shape of microtubules was changed and "9 + 2" structure was unclear in the sperm tails (Fig. 4E, F). In the combination of HFD and SiNPs treatment groups, the shape of mitochondrial has changed rapidly with the increased dosages of SiNPs. Mitochondrial cristae were hard to observe, and the mitochondria membrane was ruptured in all the HFD + SiNPs groups. In addition, among the HFD groups, the microtubules of the sperm tails showed the "9 + 2" structures were obscure with all dosages of SiNPs treatment (Fig. 4G–L).

3.7. The changes of protein expressions of meiotic regulating factors

As shown in Fig. 5, HFD intake obviously decreased the expression of Cyclin A1 ($p = 0.001$) while significantly increased the expression of CDK1 ($p = 0.021$), and no significant effect was observed on the expression of Sohlh1 ($p = 0.266$), CDK2 ($p = 0.643$) and Cyclin B1 ($p = 0.093$) when compared with the control group. SiNPs significantly decreased the expression of Sohlh1 ($p = 0.017$), CDK2 ($p = 0.017$) and Cyclin A1 ($p = 0.001$), while obviously improved the expression of CDK1 ($p = 0.007$) when compared with the control group in testicular tissue in rats. Moreover, SiNPs obviously inhibited the expression of Sohlh1, CDK2, Cyclin A1, CDK1 and Cyclin B1 in HFD groups. Among the HFD groups, 10 mg/kg·bw SiNPs could decrease the expression of sohlh1 ($p = 0.008$) and Cyclin A1 ($p = 0.004$). The levels of CDK2 and Cyclin B1 in all dosages of SiNPs dramatically reduced, and CDK1 level in 5 and 10 mg/kg·bw SiNPs group significantly lowered in HFD groups ($p < 0.01$).

4. Discussion

Consumption of high-fat diet is an unhealthy lifestyle and is likely the direct cause of obesity, which is a risk factor for many human diseases (O'Neill et al., 2016; Wires et al., 2017). Air pollution is a complex mixture of solid particles and gases, and SiNPs have been recognized as the main inorganic ingredient of air polluted sources (Duan et al., 2016; Lag et al., 2018). The most common way for human exposure to SiNPs is via the atmosphere (Liang et al., 2014). SiNPs are of special interest and found in particle matter. SiNPs in the air are mainly

Table 1
Effects of different doses of silica nanoparticles on sperm quality and quantity in high-fat diet Wistar rats.

	Sperm concentration ($\times 10^4$ mL^{-1})	Sperm motility rate (%)	Sperm abnormality rate (%)
Control	10,575.00 ± 2941.22	79.00 ± 4.30	1.87 ± 0.50
HFD	7466.67 ± 1079.66*	33.00 ± 3.32*	4.03 ± 0.45*
SiNPs (10 mg kg^{-1})	6733.33 ± 964.19*	40.60 ± 3.05*	3.57 ± 0.65*
HFD + SiNPs (2 mg kg^{-1})	3625.00 ± 830.05#	34.40 ± 3.78	4.20 ± 0.72
HFD + SiNPs (5 mg kg^{-1})	2916.67 ± 422.69#	26.40 ± 2.30#	7.63 ± 1.16#
HFD + SiNPs (10 mg kg^{-1})	3616.67 ± 553.92#	31.60 ± 5.03	8.60 ± 1.28#

* indicates remarkable difference compared with the control group, # indicates significant difference compared with the high-fat diet group. N = 10 per group, Data are expressed as means ± S.D. from three independent experiments per index. The data showed in the figure are representative. ($p < 0.05$).

from road dust, construction dust and industry (Duan et al., 2016; Feng et al., 2019; Shen et al., 2016), which are hazardous and have multiple adverse health effects on human beings (Liu et al., 2018; Leclerc et al., 2015). Some studies have proved that environmental pollutions and lifestyles changes mainly contribute to the reproductive disorders (Pacey, 2010; Barazani et al., 2014; Zhang et al., 2018). To assess the effect of HFD on semen, the quantity and quality of sperms were measured. In the current study, decreased sperm concentration, motility rates and increased abnormality rates were observed in HFD group, which suggested that HFD might be able to arouse sperm abnormity. Similar research showed that HFD-treated obese male rats and mice present a reduced percentage rate of mobile spermatozoa (Ghanayem et al., 2010; Miao et al., 2018). We found that SiNPs further reduced sperm concentration, motility rates and abnormality rates, which suggested that SiNPs contributed to aggravate the damage of testis in HFD rats. Our previous study also presented an idea that SiNPs could result in the decrease of the quantity and quality of sperm in mice (Jin Zhang et al., 2016). Continuous process of spermatogenesis in the seminiferous tubules includes transformation from undifferentiated spermatogonia to mature spermatozoa via the mitosis stage of spermatogonia as well as spermatocytes and maturation of spermatids (Nakata et al., 2015). Therefore, we quantitatively analyzed the cellular composition in seminiferous tubules in testis sections by counting the numbers of spermatogenic cells in various stages. Results suggested that HFD significantly reduced the seminiferous tubule diameter and spermatoblasts number while elevated the amount of spermatogonium, which suggested that HFD might disrupt the formation of sperm and block meiosis process in Wistar rats. Some studies showed that obesity rats induced by HFD causes adverse effects on spermatogenesis process and semen quality (Leite et al., 2018; Jia et al., 2018; Xiang et al., 2018). Besides, a study from Campos-Silva et al illustrated that seminiferous tubule diameter of Wistar rats was lower in the group treated by HFD with saturated and polyunsaturated fatty acids compared with the standard diet team (Campos-Silva et al., 2015), which was similar to our results. Moreover, SiNPs led to detrimental effect on reproductive system in HFD rats in the current experiment. We found that SiNPs reduced the number of spermatogonium, primary spermatocyte and spermatoblasts in HFD group, which demonstrated that combination of SiNPs and HFD suppressed the process of spermatogenesis more seriously than HFD treated isolated in Wistar rats (Table 2).

However, a clear understanding of how SiNPs react to the reproductive system in HFD rats, particularly at the molecular level, is still poorly understood. It has been suggested that meiosis process plays vital roles in sperm formation (Wei and Yang, 2018). The mechanism of the cellular uptake of SiNPs appears to be mediated through an active endocytosis process (Choi et al., 2010). Moreover, NPs' internalization only distributes NPs inside the cell cytoplasm by cells following endocytosis pathways and is unable to target the nucleus if NPs are bigger than few nanometers (Phonesouk et al., 2019). In the process of meiosis, spermatogenic cells could be disrupted by detrimental factors (Hou et al., 2019). To get a closer insight into the effect of HFD and SiNPs on meiosis process, we measured the protein expressions related

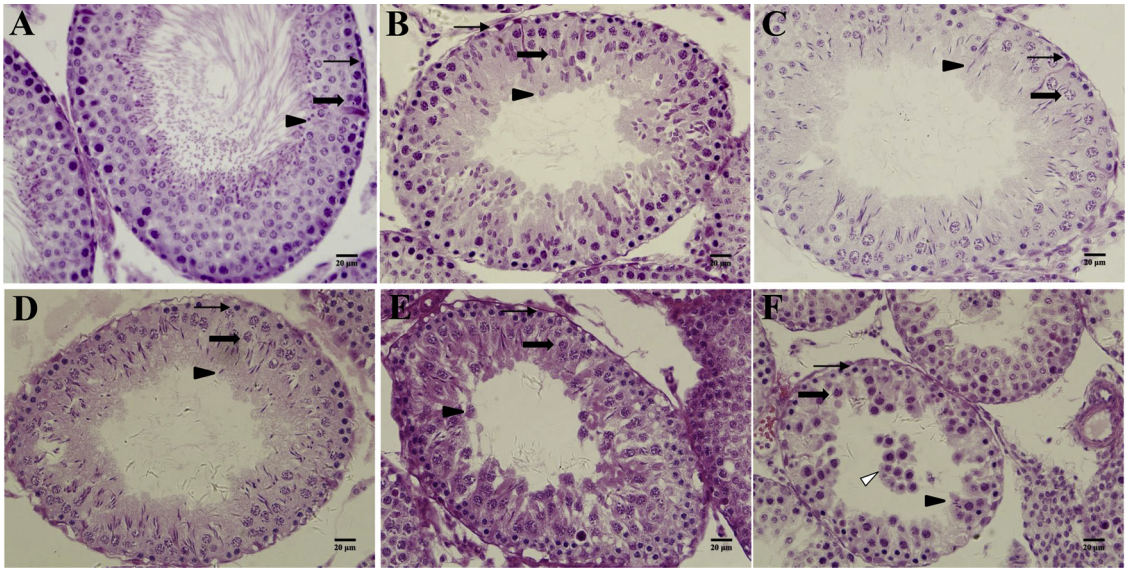

Fig. 3. Effects of different doses of silica nanoparticles (SiNPs) on structure of testicular tissue in high-fat diet (HFD) Wistar rats. (A) Control group, (B) HFD group alone, (C) 10 mg/kg·bw SiNPs group alone, (D) HFD +2 mg/kg·bw SiNPs group, (E) HFD +5 mg/kg·bw SiNPs group, (F) HFD +10 mg/kg·bw SiNPs group. Thin black arrows represent spermatogonium, thick black arrows represent primary spermatocyte, black triangles represent spermatid and the white triangle represents exfoliation of spermatogenic cells. Images were observed by an inverted phase contrast microscope (400×). N = 10 per group, Images are captured from three independent experiments. The pictures showed in the figure are representative.

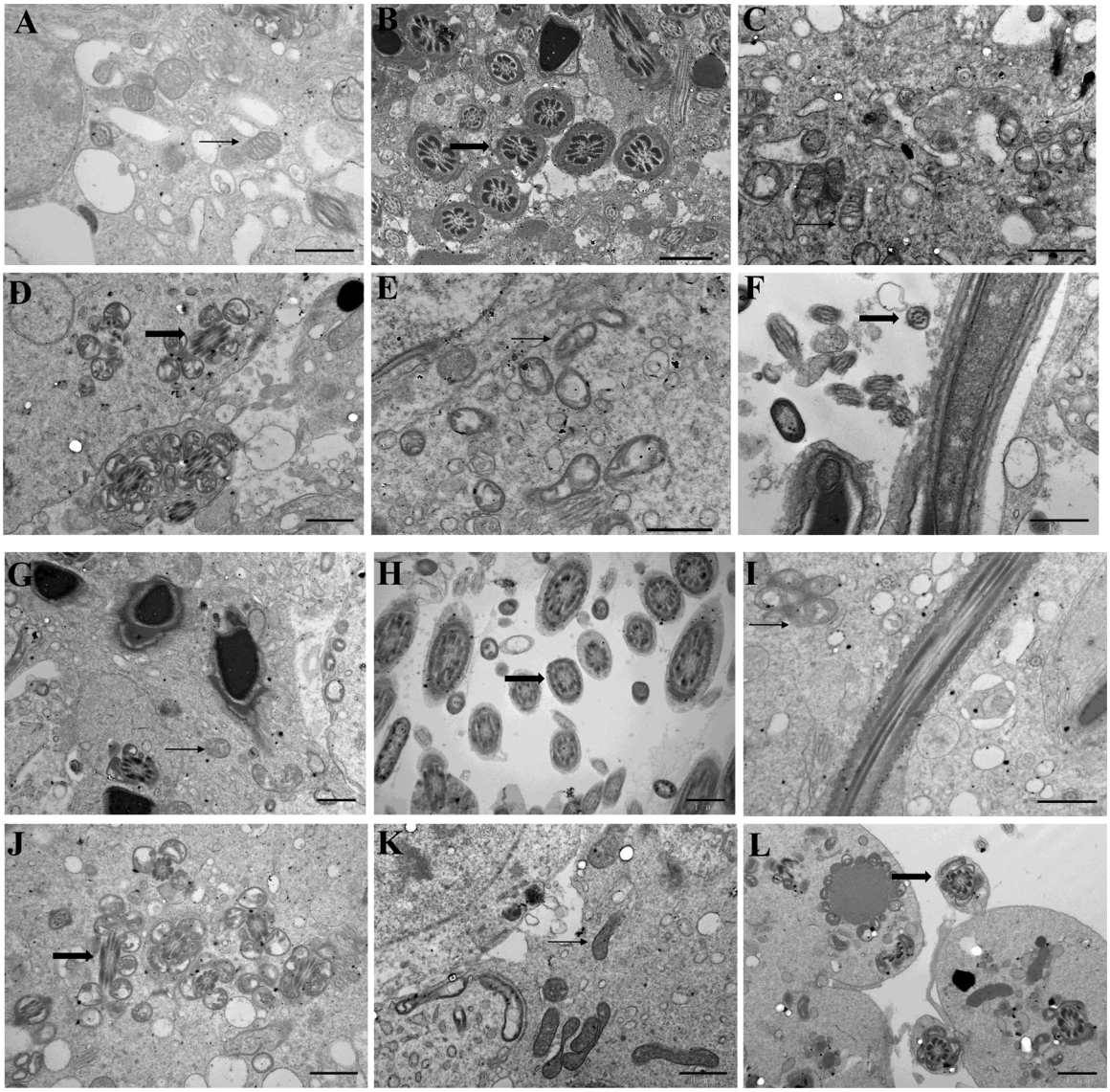

Fig. 4. Effects of different doses of silica nanoparticles (SiNPs) on ultrastructure of testicular tissue in high-fat diet (HFD) Wistar rats. (A, B) Control group, (C, D) HFD group alone, (E, F) 10 mg/kg·bw SiNPs group alone, (G, H) HFD + 2 mg/kg·bw SiNPs group, (I, J) HFD + 5 mg/kg·bw SiNPs group, (K, L) HFD + 10 mg/kg·bw SiNPs group. The thin black arrows represent mitochondria in spermatogenic cells. The wide black arrows point to the cross-sectional sperms. N = 10 per group, Images are captured from three independent experiments. The pictures showed in the figure are representative.

to process of meiosis in testicular tissues. Sohlh1 has been shown to be an essential factor for differentiation which controls start of meiosis and contribute to development of spermatophore, and SOHLH1 protein was proved to be exclusively expressed in spermatogonia (Ballow et al., 2006). Our present study found that highest dose of SiNPs could make a decrease in Sohlh1 expression in HFD rats, but no changes were found in HFD group without any treatment, which might indicate that the process of meiosis might be interfered by SiNPs. Furthermore, CDK2 kinase activity is the essential in meiotic functions in eukaryotes (Chauhan et al., 2016). CDK2 can bind to cyclin A1 and then contributes to the progress that cells passing into the metaphase of meiosis (Wolgemuth et al., 2002). Meanwhile, Cyclin B1 is activated by cyclin A1 to create a complex of CDK1/cyclin B (also called maturation promoting factor) at the meiotic phase, which shifts cells access to G2/M phage (Godet et al., 2000). Our results showed that SiNPs resulted in the significantly decreased expressions of Cyclin A1 and CDK2. Interestingly, the expression of CDK1 was significantly increased by both HFD and SiNPs. This is different from our previous study, which showed that SiNPs could decrease CDK1 expression in mice (Jin Zhang et al., 2016), which various dosage and exposed time of SiNPs responded to the different effects. The combinative effect of HFD and SiNPs could significantly reduce the expressions of Sohlh1, CDK2, Cyclin A1, CDK1 and Cyclin B1 compared with the levels in the HFD isolated group, which means that joint effect of SiNPs strongly inhibited the meiotic signaling pathway in HFD rats. Mitochondria are central hubs of energy metabolism. The main two functions of mitochondria are generating ATP and sustaining biosynthesis, which should be appropriately balanced to meet specific cellular demands (Weinberg et al., 2015; Beckervordersandforth, 2017). Thus, our results regard to ultrastructure of testis showed that HFD could damage mitochondrial structure of spermatogenic cells, and SiNPs furthered to accelerate the injury extent in the HFD groups. The damaged mitochondria might induce to energy metabolism deficiency which further explains the decrease of ATP levels and semen quality.

Though data for reproductive experiments on experimental animals' exposure to SiNPs or HFD are accessible, the relevant study on human health is still lacking. Therefore, there is a significant gap between experimental animal data and human health effects. It is necessary to

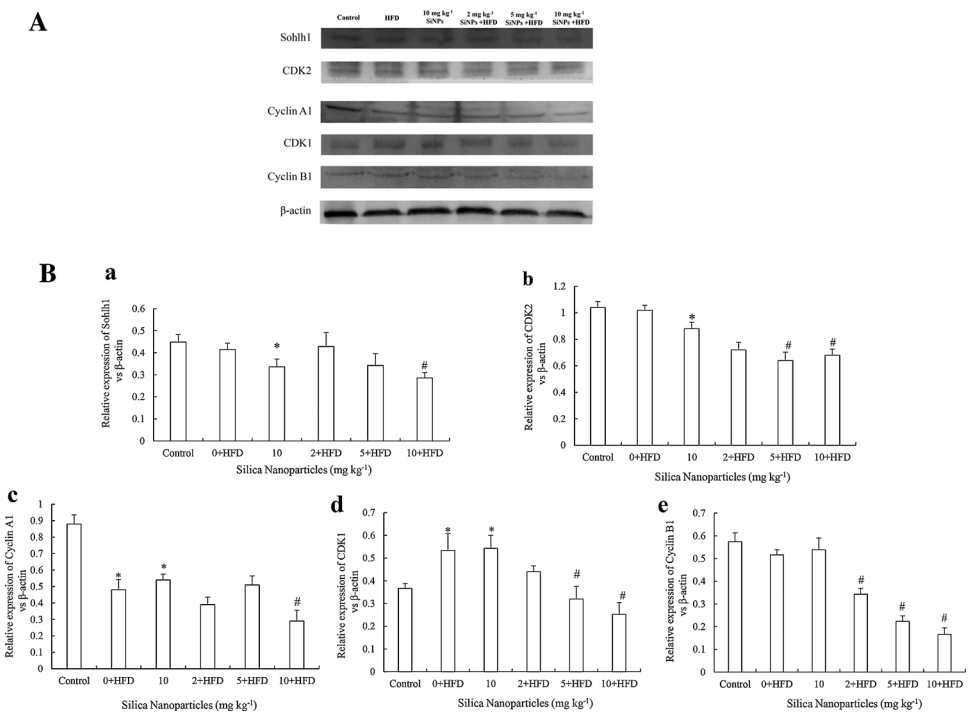

Fig. 5. Effects of different doses of silica nanoparticles (SiNPs) on the meiosis regulators of testicular tissue in high-fat diet (HFD) Wistar rats. (A) Expressions of Sohlh1, CDK2, Cyclin A1, CDK1 and Cyclin B1. (B) Relative densitometric analysis of Sohlh1 (a), CDK2 (b), Cyclin A1 (c), CDK1 (d) and Cyclin B1(e) expressions. * indicates remarkable difference compared with the control group, # indicates significant difference compared with the HFD group. N = 10 per group, Data are expressed as means ± S.D. from three independent experiments per index. The data showed in the figure are representative. ($p < 0.05$).

Table 2
Effects of different doses of silica nanoparticles on changes of diameter of the seminiferous tubule and the number of spermatogenic cells in high-fat diet Wistar rats.

	Control	HFD	SiNPs (10 mg kg^{-1})	HFD + SiNPs (2 mg kg^{-1})	HFD + SiNPs (5 mg kg^{-1})	HFD + SiNPs (10 mg kg^{-1})
Seminiferous tubule diameter (μm)	310.89 ± 29.12	240.11 ± 31.33*	313.00 ± 27.21	247.54 ± 32.47	253.56 ± 39.80	240.82 ± 31.75
Spermatogonium(number)	43.00 ± 6.13	57.33 ± 8.64*	37.52 ± 4.74*	44.79 ± 6.43#	47.77 ± 6.03#	51.60 ± 7.76
Primary spermatocyte (number)	51.83 ± 13.94	52.86 ± 8.75	48.43 ± 12.63	43.7 ± 7.49#	48.07 ± 7.57	52.46 ± 12.33
Spermatoblasts (number)	133.33 ± 10.66	112.24 ± 8.76*	100.22 ± 9.03*	87.7 ± 7.49#	81.57 ± 9.04#	86.11 ± 7.70#

* indicates remarkable difference compared with the control group, # indicates significant difference compared with the high-fat diet group. N = 10 per group, Data are expressed as means ± S.D. from three independent experiments per index. The data showed in the figure are representative. ($p < 0.05$).

strengthen the development of transformational toxicology. Transforming the findings of basic toxicology research into the medical indexes for measurement of human risk should be focused on in the future. Besides, more molecular biomarkers can be screened out to the benefit of assessment of adverse health effects with the intensive study of toxicity mechanism of SiNPs.

5. Conclusion

The present study illustrated that both HFD and SiNPs decreased the quality and quantity of sperms, damaged testicular structure, reduced ATP level and affected expressions of regulatory factors of meiosis in testis of Wistar rats. The combination of HFD and SiNPs further decreased the sperm concentration, sperm motility rate, elevated sperm abnormality rate, aggravated the structural destruction of testis, lowered the ATP level and expressions of Sohlh1, CDK2, Cyclin A1, CDK1 and Cyclin B1 associated with meiotic signaling pathway compared with the HFD in isolation in testicular tissue of Wistar rats. SiNPs could inhibit the start of meiosis and spermatophore development by down-regulating the expression of Sohlh1, cyclin A1, CDK1, and CDK2, which inhibits the meiosis process, thereby decreasing the amount of sperm in HFD rats. In addition, SiNPs could reduce sperm motility via the ATP decrease resulting from the damage of mitochondria in HFD rats. Meanwhile, SiNPs might disrupt the structure of sperm and increase sperm abnormality rates in HFD rats. These results suggested that SiNPs significantly promoted reproductive toxicity induced by HFD in Wistar rats. Further study is necessary to explore the underlying effect mechanisms on how SiNPs acted on the HFD rats that intensified the reproductive toxicity.

Acknowledgments

This study was supported by Beijing Municipal Natural Science Foundation Program and the Scientific Research Key Program of Beijing Municipal Commission of Education (KZ201510025028).

References

Duan, J., Yu, Y., Li, Y., Wang, Y., Sun, Z., 2016. Inflammatory response and blood hypercoagulable state induced by low level co-exposure with silica nanoparticles and benzo[a]pyrene in zebrafish (Danio rerio) embryos. Chemosphere 151, 152–162.
Feng, L., Yang, X., Liang, S., Xu, Q., Miller, M.R., Duan, J., Sun, Z., 2019. Silica nanoparticles trigger the vascular endothelial dysfunction and prethrombotic state via miR-451 directly regulating the IL6R signaling pathway. Part. Fibre Toxicol. 16, 16.
Shen, Z., Sun, J., Cao, J., Zhang, L., Zhang, Q., Lei, Y., Gao, J., Huang, R.J., Liu, S., Huang, Y., Zhu, C., Xu, H., Zheng, C., Liu, P., Xue, Z., 2016. Chemical profiles of urban fugitive dust PM2.5 samples in Northern Chinese cities. Sci. Total Environ. 569-570, 619–626.
Liu, J., Yang, M., Jing, L., Ren, L., Wei, J., Zhang, J., Zhang, F., Duan, J., Zhou, X., Sun, Z., 2018. Silica nanoparticle exposure inducing granulosa cell apoptosis and follicular atresia in female Balb/c mice. Environ. Sci. Pollut. Res. Int. 25, 3423–3434.
Sengupta, P., Dutta, S., Krajewska-Kulak, E., 2017. The disappearing sperms: analysis of reports published between 1980 and 2015. Am. J. Men's Health 11, 1279–1304.
Lafuente, R., Garcia-Blaquez, N., Jacquemin, B., Checa, M.A., 2016. Outdoor air pollution and sperm quality. Fertil. Steril. 106, 880–896.
Agarwal, A., Mulgund, A., Hamada, A., Chyatte, M.R., 2015. A unique view on male

infertility around the globe. Reprod. Biol. Endocrinol. 13, 37.
Miura, N., Ohtani, K., Hasegawa, T., Yoshioka, H., Hwang, G.W., 2017. High sensitivity of testicular function to titanium nanoparticles. J. Toxicol. Sci. 42, 359–366.
Baki, M.E., Miresmaili, S.M., Pourentezari, M., Amraii, E., Yousefi, V., Spenani, H.R., Talebi, A.R., Anvari, M., Fazilati, M., Fallah, A.A., Mangoli, E., 2014. Effects of silver nano-particles on sperm parameters, number of Leydig cells and sex hormones in rats. Iran. J. Reprod. Med. 12, 139–144.
Xu, Y., Wang, N., Yu, Y., Li, Y., Li, Y.B., Yu, Y.B., Zhou, X.Q., Sun, Z.W., 2014. Exposure to silica nanoparticles causes reversible damage of the spermatogenic process in mice. PLoS One 9 e101572.
Deshpande, S., Rigby, M.J., Blair, M., 2018. The presence of eHealth support for childhood obesity guidance. Stud. Health Technol. Inform. 247, 945–949.
Luo, K., Bian, J., Wang, Q., Wang, J., Chen, F., Li, H., Jin, D., 2019. Association of obesity with chronic kidney disease in elderly patients with nonalcoholic fatty liver disease. Turk. J. Gastroenterol. 30, 611–615.
Li, Y.R., Ro, V., Tchou, J.C., 2018. Obesity, metabolic syndrome, and breast cancer: from prevention to intervention. Curr. Surg. Rep. 6.
Zhang, H., Zhou, L., 2019. Single nucleotide polymorphism of PIK3CA and its interaction with the environment are risk factors for Chinese Han ovarian cancer. Pathol. Res. Pract., 152520.
Aiceles, V., da Fonte Ramos, C., 2016. A link between hypothyroidism, obesity and male reproduction. Horm. Mol. Biol. Clin. Investig. 25, 5–13.
Paoli, D., Pecora, G., Pallotti, F., Faja, F., Pelloni, M., Lenzi, A., Lombardo, F., 2019. Cytological and molecular aspects of the ageing sperm. Hum. Reprod. 34, 218–227.
Mao, G., Nachman, R.M., Sun, Q., Zhang, X., Koehler, K., Chen, Z., Hong, X., Wang, G., Caruso, D., Zong, G., Pearson, C., Ji, H., Biswal, S., Zuckerman, B., Wills-Karp, M., Wang, X., 2016. Individual and joint effects of early-life ambient PM2.5 exposure and maternal pre-pregnancy obesity on childhood overweight or obesity. Environ. Health Perspect.
Aggerholm, A.S., Thulstrup, A.M., Toft, G., Ramlau-Hansen, C.H., Bonde, J.P., 2008. Is overweight a risk factor for reduced semen quality and altered serum sex hormone profile? Fertil. Steril. 90, 619–626.
Valbuena, G., Hernandez, F., Madrid, J.F., Saez, F.J., 2008. Acrosome biosynthesis in spermatocytes and spermatids revealed by HPA lectin cytochemistry. Anat. Rec. 291, 1097–1105.
Walker, W.H., Cheng, J., 2005. FSH and testosterone signaling in Sertoli cells. Reproduction 130, 15–28.
Matson, C.K., Murphy, M.W., Griswold, M.D., Yoshida, S., Bardwell, V.J., Zarkower, D., 2010. The mammalian doublesex homolog DMRT1 is a transcriptional gatekeeper that controls the mitosis versus meiosis decision in male germ cells. Dev. Cell 19, 612–624.
Ballow, D., Meistrich, M.L., Matzuk, M., Rajkovic, A., 2006. Sohlh1 is essential for spermatogonial differentiation. Dev. Biol. 294, 161–167.
Campsteijn, C., Ovrebo, J.I., Karlsen, B.O., Thompson, E.M., 2012. Expansion of cyclin D and CDK1 paralogs in Oikopleura dioica, a chordate employing diverse cell cycle variants. Mol. Biol. Evol. 29, 487–502.
Guo, F.Z., Zhang, L.S., Wei, J.L., Ren, L.H., Zhang, J., Jing, L., Yang, M., Wang, J., Sun, Z.W., Zhou, X.Q., 2016. Endosulfan inhibiting the meiosis process via depressing expressions of regulatory factors and causing cell cycle arrest in spermatogenic cells. Environ. Sci. Pollut. Res. Int. 23, 20506–20516.
Du, Z., Zhao, D., Jing, L., Cui, G., Jin, M., Li, Y., Liu, X., Liu, Y., Du, H., Guo, C., Zhou, X., Sun, Z., 2013. Cardiovascular toxicity of different sizes amorphous silica nanoparticles in rats after intratracheal instillation. Cardiovasc. Toxicol. 13, 194–207.
Kim, M.J., Jung, H.N., Kim, K.N., Kwak, H.K., 2008. Effects of cranberry powder on serum lipid profiles and biomarkers of oxidative stress in rats fed an atherogenic diet. Nutr. Res. Pract. 2, 158–164.
Guo, C., Xia, Y., Niu, P., Jiang, L., Duan, J., Yu, Y., Zhou, X., Li, Y., Sun, Z., 2015. Silica nanoparticles induce oxidative stress, inflammation, and endothelial dysfunction in vitro via activation of the MAPK/Nrf2 pathway and nuclear factor-kappaB signaling. Int. J. Nanomed. 10, 1463–1477.
Melvin, A., Vijay, R., Chaudhari, V.R., Gupta, B., Prakash, R., Haram, S., Baskar, G., Khushalani, D., 2010. A facile methodology for the design of functionalized hollow silica spheres. J. Colloid Interface Sci. 346, 265–269.
Martins, M.R., Silva, J.R., 2001. Ultrastructure of spermatogonia and primary spermatocytes of C57BL6J mice. Anat. Histol. Embryol. 30, 129–132.
Jin Zhang, L.R., Zou, Yang, Zhang, Lianshuang, Wei, Jialiu, Li, Yanbo, Ji, Wang, Sun, Zhiwei, Zhou, Xianqing, 2016. Silica nanoparticles induce start inhibition of meiosis and cell cycle arrest via down-regulating meiotic relevant factors. Toxicol. Res. 5, 1453–1464.
O'Neill, A.M., Burrington, C.M., Gillaspie, E.A., Lynch, D.T., Horsman, M.J., Greene, M.W., 2016. High-fat Western diet-induced obesity contributes to increased tumor growth in mouse models of human colon cancer. Nutr. Res. 36, 1325–1334.
Wires, E.S., Trychta, K.A., Back, S., Sulima, A., Rice, K.C., Harvey, B.K., 2017. High fat diet disrupts endoplasmic reticulum calcium homeostasis in the rat liver. J. Hepatol. 67, 1009–1017.
Lag, M., Skuland, T., Godymchuk, A., Nguyen, T.H.T., Pham, H.L.T., Refsnes, M., 2018. Silica nanoparticle-induced cytokine responses in BEAS-2B and HBEC3-KT cells: significance of particle size and signalling pathways in different lung cell cultures. Basic Clin. Pharmacol. Toxicol. 122, 620–632.
Liang, X., Chen, W., Sun, G., Liu, S., Cai, H., Zhou, L., 2014. Experimental study on new self and mutual-aiding occlusive dressing for wound. Chin. Med. J. (Engl.) 127, 1321–1327.
Leclerc, L., Klein, J.P., Forest, V., Boudard, D., Martini, M., Pourchez, J., Blanchin, M.G., Cottier, M., 2015. Testicular biodistribution of silica-gold nanoparticles after intramuscular injection in mice. Biomed. Microdev. 17, 66.
Pacey, A.A., 2010. Environmental and lifestyle factors associated with sperm DNA damage. Hum. Fertil. 13, 189–193.
Barazani, Y., Katz, B.F., Nagler, H.M., Stember, D.S., 2014. Lifestyle, environment, and male reproductive health. Urol. Clin. North Am. 41, 55–66.
Zhang, M., Mueller, N.T., Wang, H., Hong, X., Appel, L.J., Wang, X., 2018. Maternal exposure to ambient particulate matter < /=2.5 microm during pregnancy and the risk for high blood pressure in childhood. Hypertension.
Ghanayem, B.I., Bai, R., Kissling, G.E., Travlos, G., Hoffler, U., 2010. Diet-induced obesity in male mice is associated with reduced fertility and potentiation of acrylamide-induced reproductive toxicity. Biol. Reprod. 82, 96–104.
Miao, X.L., Gao, G.M., Jiang, L., Xu, R., Wan, D.P., 2018. Asiatic acid attenuates high-fat diet-induced impaired spermatogenesis. Exp. Ther. Med. 15, 2397–2403.
Nakata, H., Wakayama, T., Takai, Y., Iseki, S., 2015. Quantitative analysis of the cellular composition in seminiferous tubules in normal and genetically modified infertile mice. J. Histochem. Cytochem. 63, 99–113.
Leite, G.A.A., Sanabria, M., Cavariani, M.M., Anselmo-Franci, J.A., Pinheiro, P.F.F., Domeniconi, R.F., Kempinas, W.G., 2018. Lower sperm quality and testicular and epididymal structural impairment in adult rats exposed to rosuvastatin during prepuberty. J. Appl. Toxicol. 38, 914–929.
Jia, Y.F., Feng, Q., Ge, Z.Y., Guo, Y., Zhou, F., Zhang, K.S., Wang, X.W., Lu, W.H., Liang, X.W., Gu, Y.Q., 2018. Obesity impairs male fertility through long-term effects on spermatogenesis. BMC Urol. 18, 42.
Xiang, J., Bian, C., Wan, X., Zhang, Q., Huang, S., Wu, D., 2018. Sleeve gastrectomy reversed obesity-induced hypogonadism in a rat model by regulating inflammatory responses in the hypothalamus and testis. Obes. Surg.
Campos-Silva, P., Furriel, A., Costa, W.S., Sampaio, F.J., Gregorio, B.M., 2015. Metabolic and testicular effects of the long-term administration of different high-fat diets in adult rats. Int. Braz. J. Urol. 41, 569–575.
Wei, Y.L., Yang, W.X., 2018. The acroframosome-acroplaxome-manchette axis may function in sperm head shaping and male fertility. Gene 660, 28–40.
Choi, J., Zheng, Q., Katz, H.E., Guilarte, T.R., 2010. Silica-based nanoparticle uptake and cellular response by primary microglia. Environ. Health Perspect. 118, 589–595.
Phonesouk, E., Lechevallier, S., Ferrand, A., Rols, M.P., Bezombes, C., Verelst, M., Golzio, M., 2019. Increasing uptake of silica nanoparticles with electroporation: from cellular characterization to potential applications. Materials 12.
Hou, X., Zhu, L., Zhang, X., Zhang, L., Bao, H., Tang, M., Wei, R., Wang, R., 2019. Testosterone disruptor effect and gut microbiome perturbation in mice: early life exposure to doxycycline. Chemosphere 222, 722–731.
Chauhan, S., Diril, M.K., Lee, J.H., Bisteau, X., Manoharan, V., Adhikari, D., Ratnacaram, C.K., Janela, B., Noffke, J., Ginhoux, F., Coppola, V., Liu, K., Tessarollo, L., Kaldis, P., 2016. Cdk2 catalytic activity is essential for meiotic cell division in vivo. Biochem. J. 473, 2783–2798.
Wolgemuth, D.J., Laurion, E., Lele, K.M., 2002. Regulation of the mitotic and meiotic cell cycles in the male germ line. Recent Prog. Horm. Res. 57, 75–101.
Godet, M., Thomas, A., Rudkin, B.B., Durand, P., 2000. Developmental changes in cyclin B1 and cyclin-dependent kinase 1 (CDK1) levels in the different populations of spermatogenic cells of the post-natal rat testis. Eur. J. Cell Biol. 79, 816–823.
Weinberg, S.E., Sena, L.A., Chandel, N.S., 2015. Mitochondria in the regulation of innate and adaptive immunity. Immunity 42, 406–417.
Beckervordersandforth, R., 2017. Mitochondrial metabolism-mediated regulation of adult neurogenesis. Brain Plast. 3, 73–87.